International Journal of Information, Control and Computer Sciences
ISSN: 2517-9942
Vol:4, No:3, 2010

Improved Feature Processing for Iris Biometric Authentication System

Somnath Dey and Debasis Samanta

***Abstract*—**Iris-based biometric authentication is gaining importance in recent times. Iris biometric processing however, is a complex process and computationally very expensive. In the overall processing of iris biometric in an iris-based biometric authentication system, feature processing is an important task. In feature processing, we extract iris features, which are ultimately used in matching. Since there is a large number of iris features and computational time increases as the number of features increases, it is therefore a challenge to develop an iris processing system with as few as possible number of features and at the same time without compromising the correctness. In this paper, we address this issue and present an approach to feature extraction and feature matching process. We apply Daubechies D_4 wavelet with 4 levels to extract features from iris images. These features are encoded with 2 bits by quantizing into 4 quantization levels. With our proposed approach it is possible to represent an iris template with only 304 bits, whereas existing approaches require as many as 1024 bits. In addition, we assign different weights to different iris region to compare two iris templates which significantly increases the accuracy. Further, we match the iris template based on a weighted similarity measure. Experimental results on several iris databases substantiate the efficacy of our approach.

***Keywords*—**Iris recognition, biometric, feature processing, pattern recognition, pattern matching.

I. Introduction

Recent advances in information technology and increasing emphasis on security have resulted in more attention to automatic personal identification system based on biometrics. Biometric technology is an automated method for recognizing an individual based on physiological or behavioral characteristics. Among the present biometric traits, iris is found to be the most reliable and accurate [1] due to the rich texture of iris patterns, persistence of features through the life time of an individual and it is neither duplicable nor imitable. These characteristics make it more attractive for used as a biometric feature to identify individuals.

In iris biometric system, an important task is to extract iris feature from a given eye image. In an eye image of a person, iris is an annular part between the pupil and the white sclera (see Figure 1). The iris part has a number of characteristics such as freckles, corneas, stripe, furrows, crypts etc. which constitutes what is called iris features. Since iris features are distinct from one person to another, these are considered in iris-based recognition process. Human iris recognition process is basically divided into two phases. The phase, which is dealt with the extraction of iris features from an eye image and store them into database is called the "enrollment process". At the time of matching we capture the iris features of a human and compare it with the stored features, which is called the "matching process". Each of the above phases are complex and hence is divided into several sub tasks. Figure 2 shows the different steps involved in the two phases. First four tasks in both the phases are common as it is evident in Figure 2. The task namely, "matching features" is extra in the matching process. Among all these tasks feature processing is the most important task in an iris-based biometric authentication system sofar the overall performance of an iris-based biometric authentication system is concerned.

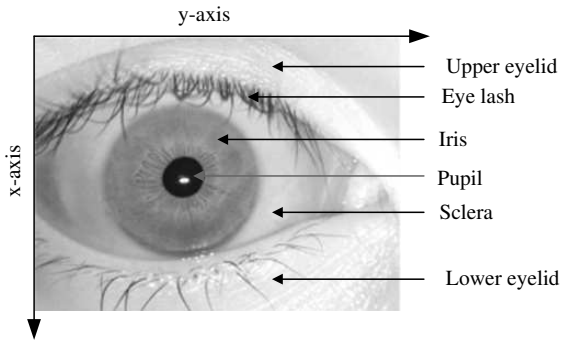

Fig. 1. The typical components in an eye image.

The feature processing task is basically composed of two sub tasks: feature extraction and feature encoding. In the feature extraction task, we capture the discriminant iris features from a normalized iris image. There are several methods to capture the iris features. Gabor filter is used in several works [1], [2], [3]. In [4], zero crossing wavelet transform is used to extract the iris features. The other methods for iris feature extraction include Log-Gabor wavelet [5], Haar wavelet [6], [7], Laplacian-of-Gaussian filter [8], Gaussian-Hermitte moments [9] etc. It is reviewed that the number of extracted iris features in the existing work is very high. The existing approaches require higher number of bits to represent the iris features and as a consequence the need of higher computations to process these iris features. In this paper, we have addressed this limitation. We focus on reducing the number of iris features without compromising the accuracy rate. We also propose an encoding scheme to store an iris feature with a lesser number of bits.

In our approach, we divide a normalized iris image into eight sub-images and apply Daubechies D_4 wavelet to extract the iris features. To encode the iris features we use four level quantization technique. We also develop a weighted matching

Somnath Dey is with the School of Information Tchnology, Indian Institute of Technology, Kharagpur, India-721302, email: somnath@sit.iitkgp.ernet.in
Debasis Samanta is with the School of Information Tchnology, Indian Institute of Technology, Kharagpur, India-721302, email: dsamanta@iitkgp.ac.in

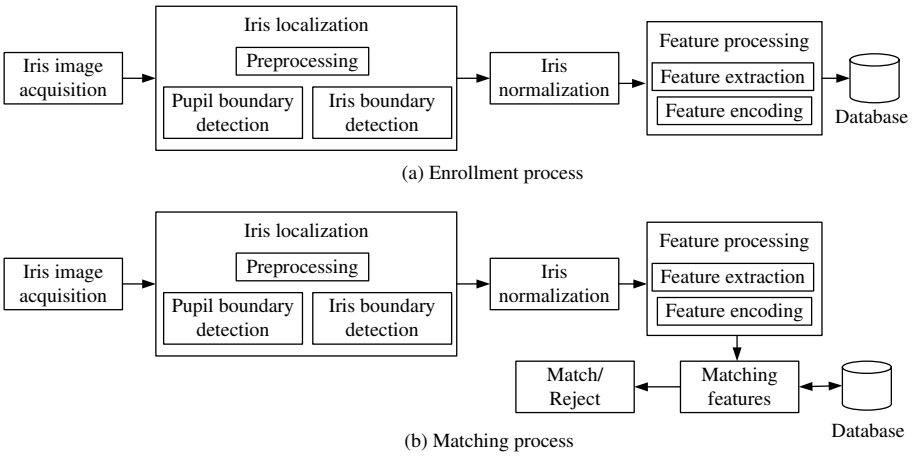

Fig. 2. Two basic processes in iris recognition.

technique to measure the similarity between any two iris feature templates.

The rest of the paper is organized as follows. In Section II, we discuss the related work. Section III presents our proposed approach to capture iris features from a normalized image and matching technique. In Section IV, we give the implementation of our approach and experimental results. Finally, the paper is concluded in Section V.

II. Related Work

The iris feature extraction process is roughly divided into three major categories: the phase-based method [1], [2], [3], [5], [10], zero-crossing representation [4] and texture analysis based method [8], [11], [9], [12], [6], [13], [14], [7]. The well-known phase based methods for feature processing are Gabor wavelet, Log-Gabor wavelet. The 1 D wavelet is known for the zero-crossing representation. The Laplacian of Gaussian filter and Gaussian-Hermite moments are used in texture analysis based method.

Daugman [1], [2], [3] uses the 2D version of Gabor filters [15], [16] to extract the iris features and demodulates the output of the Gabor filters in order to compress the data. Demodulation is done by quantizing the phase information into four levels for each possible quadrant in the complex plane. These four levels are represented using two bits of data. In other words, each pixel in the normalized iris pattern corresponds to two bits of data in the iris template. A total of 2,048 bits are calculated for the template, and an equal number of masking bits are generated in order to mask out corrupted regions within the iris. This creates a compact 256-byte template. Vasta et al. [5] use Log-Gabor filter for iris feature extraction. Boles and Boashash [4] calculated zero-crossing representation of 1D wavelet transform at various resolution levels of a virtual circle of an iris image to characterize the texture of the iris. Wildes et al. [8] represented the iris texture with a Laplacian of Gaussian filter constructed with four different resolution levels. L. Ma et al. [9] use Gaussian-Hermite moments to characterize local variations of the intensity signals. Gaussian-Hermite moments are used for texture feature extraction with mathematical orthogonality and effectiveness for characterizing local details of the signal [17]. Lim et al. [7] and Ali et al. [6] decomposed an iris image into four levels using 2D Haar wavelet transform and quantized the fourth-level high-frequency information to form an 87-bit code. L. Ma et al. [11], [18], [12] constructed a bank of spatial filters, whose kernels are suitable for iris recognition to represent local texture features of the iris and thus achieved much better results. The one-dimensional continuous wavelet transform is used to decompose iris image in [13]. Here, each decomposed one-dimensional waveform is approximated by an optimal piecewise linear curve connecting a small set of node points, which is used as a feature vector.

There are several matching techniques [3], [5], [1], [11], [6], [14] to match a captured iris template with enrolled template. Among all these Hamming distance, Weighted Euclidean distance [14] and Normalized correlation [8] measurement techniques are papular. The Hamming distance gives a measure of how many bits are same between two bit patterns. The Hamming distance (HD) [3] via the XOR operator is used for the similarity measure between two iris templates in [3], [5], [1], [19], [11], [6]. The Weighted Euclidean distance (WED) is used to compare two iris templates in [14]. The weighted Euclidean distance gives a measure of how similar a collection of values are between two templates. The weighted Euclidean distance can be used to compare two templates, especially if the template is composed of integer values. The normalized correlation is for matching the iris template and was used by Wildes et al. [8] and Kim et al. [13].

III. Proposed Approach

The feature processing task is followed by two iris preprocessing tasks namely, iris localization [20] and iris normalization [20] of an input eye image. In this work, we consider that the normalized eye image is available accurately following the above mentioned preprocessing tasks. We consider the preprocessing approach proposed in [20] to localize the iris part and store it in normalized form (see Figure 3). Further to deal with eye images with inferior quality, we follow

the enhancement techniques proposed in [20]. We could not incorporate the above mentioned preprocessing tasks because of the page limitation.

The feature processing task consists of two sub tasks namely, feature extraction and feature encoding. In this section, we discus our approach to feature extraction and feature encoding. Our approach to feature extraction considers Daubechies wavelet transform, which we first mention for the convenience of the reader followed by our approach to the two tasks of feature processing.

A. Daubechies Wavelet Transform

Wavelet transform is a popular approach to signal analysis and has been widely used in image processing [21]. It is faster as compared to the conventional signal processing algorithm based on the Fourier transform, and it can efficiently accomplish signal localization in time and frequency domains. In this sub section, we present the discrete version of Daubechies D_4 wavelet and its lifting scheme representation.

The Daubechies D_4 transform has four scaling (low-pass filter) and wavelet (high-pass filter) function coefficients. The scaling function coefficients are defined in Equation (1).

$$\begin{aligned} h_0 &= \frac{1+\sqrt{3}}{4\sqrt{2}} \qquad h_1 = \frac{3+\sqrt{3}}{4\sqrt{2}} \\ h_2 &= \frac{3-\sqrt{3}}{4\sqrt{2}} \qquad h_3 = \frac{1-\sqrt{3}}{4\sqrt{2}} \end{aligned} \tag{1}$$

Each step of the wavelet transform applies the scaling function to the data input. If the original data set has N values, the scaling function will be applied in the wavelet transform step to calculate $N/2$ smoothed values. In the ordered wavelet transform the smoothed values are stored in the lower half of the N element input vector. The wavelet function coefficient values are defined in Equation (2).

$$\begin{aligned} g_0 &= h_3 \qquad g_1 = -h_2 \\ g_2 &= h_1 \qquad g_3 = -h_0 \end{aligned} \tag{2}$$

The scaling and wavelet functions are calculated by taking the inner product of the coefficients and four data values. The Equations (3a) and (3b) are used to calculate the scaling and wavelet functions, respectively.

$$a_i = h_0\ S_{2i} + h_1\ S_{2i+1} + h_2\ S_{2i+2} + h_3\ S_{2i+3} \tag{3a}$$

$$c_i = g_0\ S_{2i} + g_1\ S_{2i+1} + g_2\ S_{2i+2} + g_3\ S_{2i+3} \tag{3b}$$

Each iteration in the wavelet transform step calculates a scaling function value and a wavelet function value. The index i is incremented by two with each iteration, and new scaling and wavelet function values are calculated.

Daubechies wavelet functions [22] are continuous functions and the characteristic values can be extracted more accurately. Therefore, in case where the images are to be again decompressed after they have been compressed by using the Daubechies wavelet transform, the images can be restored in high resolution nearer to the original images. The Daubechies wavelets have the greater number of vanishing moments properties which means better smoothness. The wavelet transform is also easy to put into practice using the fast wavelet transform. Daubechies wavelets are widely used in solving a broad range of problems, e.g. self-similarity properties of a signal or fractal problems, signal discontinuities etc.

Since Daubechies wavelet functions [22] are continuous functions, the disadvantages of the Haar wavelet functions that the values thereof are discontinuous and rapidly changes can be avoided, and the characteristic values can be extracted more accurately. The Daubechies wavelet transform also reduces the dimension of the characteristics vector.

B. Feature Extraction

In this work, we use Daubechies wavelet transform to extract characteristic values of the iris images, and it is a technique of analyzing signals in multi-resolution mode. Given a normalized (and enhanced) iris part of an eye image as a fixed block of size 64×512 pixel^2, we first divide it into eight sub images and then apply Daubechies four coefficient wavelet transform to each sub image. In other words, to extract the characteristic values in the iris image we apply Daubechies wavelet transform to eight images of size 32×128 at four different levels successively as shown in Figure 4. We extract the iris features in each sub image which includes the high frequency components in the multi-divided image for each sub images. The level of division, that is, the iterative number should be set as a proper value in consideration to loss of information and the size of the characteristic vector. The Daubechies wavelet function with eight, sixteen or more coefficients can extract more sensitive characteristic values than the Daubechies wavelet function with four coefficients, even though the former is more complicated than the later. The Daubechies wavelet function with eight or more coefficients has been used and tested in our experiment but, we could not

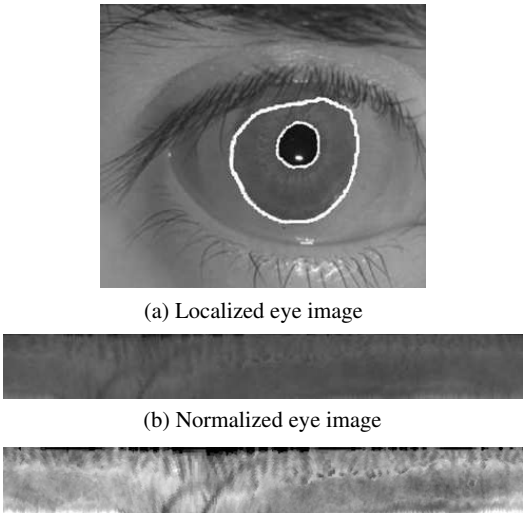

(a) Localized eye image

(b) Normalized eye image

(c) Enhanced normalized image

Fig. 3. Normalized eye image from an input eye image.

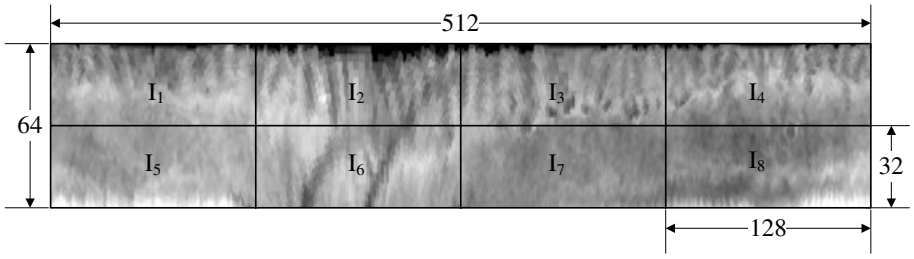

Fig. 4. Partitioning of a normalized iris image.

achieve greater performance improvement rather, processing time is increased compared to the case where the Daubechies wavelet function with four coefficients. This guides us to apply the Daubechies wavelet function with four coefficients to extract the characteristic values from the normalized iris image.

Figure 5 shows an example of multi-dividing the iris image through the Daubechies wavelet transform with four coefficients. In Figure 5, "L" and "H" are used to indicate low frequency and high frequency components, respectively. The term "LL" means a component that has passed through a low-pass filter (LPF) in all *x*- and *y*- directions whereas a term "HH" means a component that has passed through a high-pass filter (HPF) in the *x*- and *y*- directions. Furthermore, subscript numerals signify image dividing stages. For example, "LH_2" means that the image has passed through the low-pass filter in the *x*- direction and through the high-pass filter in the *y*- direction during 2-stage wavelet division.

The iris image is considered as a two-dimensional signal in which one-dimensional signals are arrayed in the *x*- and *y*- directions. The quarterly divided components of one image should be extracted by passing through the LPF and HPF in all *x*- and *y*- directions in order to analyze the iris image. That is, a two-dimensional image signal is wavelet-transformed in horizontal and vertical directions, and the image is divided into four regions LL, HL, LH, and HH after the wavelet transform has been performed once. LL region contains only low frequency components in the *x*- and *y*- directions in the multi-divided iris image. Since the extracted region LL (corresponding to the image reduced in a fourth size as compared with the previous image) includes major information on the iris image, it is provided as an image to be newly processed so that the wavelet transform can be again applied to the relevant region.

The Daubechies wavelet transform is repeatedly performed in order to reduce information sizes. In this way, the characteristic values of further reduced regions such as HH_2, HH_3 and HH_4 are obtained.

In our work, the region HH_4 for each sub images obtained by performing the wavelet transform four times which is considered as a major characteristic region. We consider the values of HH_4 region of each sub images as components of the characteristic vector. At this time, the region HH_4 contains the information having 2×8 = 16 data for each sub images. We extracted the characteristic vector of size N from the regions HH_1, HH_2, HH_3, and HH_4. In order to acquire the characteristic information on the regions HH_1, HH_2 and HH_3 excluding the information on the region HH_4 obtained through the last wavelet transform among the N characteristic vector, each average value of the regions HH_1, HH_2 and HH_3 are calculated and assigned one dimension. All the values of the region HH_4 are extracted as the characteristic values thereof. This procedure is applied to each sub image.

Let F be the characteristic vector and f^i be the feature vector of the i^{th} sub image. The F and f^i are obtained using Equation (4).

$$\begin{aligned} F &= \{\ f^1,\ f^2,\ \ldots,\ f^8\ \} \\ f^i &= \{\ f_1,\ f_2,\ \ldots,\ f_{19}\ \} \quad \text{for } i = 1, 2, \ldots, 8 \end{aligned} \tag{4}$$

The total number of characteristics values obtained for the entire normalized image is $(2 \times 8 + 3) \times 8 = 152$.

C. Feature Encoding

We generate a binary feature vector by quantizing the relevant characteristic values of a characteristic vector from the extracted image including the high frequency components in the fourth level. In the previous sub section, we obtain the characteristics vector of 152 dimensions. Now, we encode this characteristic vector to obtain feature vector. To improve the recognition rate and reduce the loss of information, we quantize a characteristic value with four levels of quantization. In this way, we not only consider the signs of characteristic values but also consider magnitude of the characteristic values using a 4-level quantization process. It requires 2-bit to encode each characteristic value. Therefore, the generated feature vector requires 304 bits (=152 ×2). Since the values of feature vectors lie in the range of -1 and +1 both inclusive, we propose to quantize these values as binary feature vectors. The binary feature vector is obtained according to Equation (5a) and Equation (5b).

$$f^n_{new_i} = \begin{cases} 11 & if \quad f^n_i \geq 0.5 \\ 10 & if \quad 0.5 > f^n_i \geq 0 \\ 01 & if \quad 0 > f^n_i \geq -0.5 \\ 00 & if \quad f^n_i \leq -0.5 \end{cases} \tag{5a}$$

where i= 1, 2, …, 19 and n = 1, 2, …, 8

$$\begin{aligned} F_{new} \quad = \quad & \{\ f^1_{new_1},\ f^1_{new_2},\ \ldots,\ f^1_{new_{19}}; \\ & f^2_{new_1},\ f^2_{new_2},\ \ldots,\ f^2_{new_{19}}; \\ & \ldots; \\ & f^8_{new_1},\ f^8_{new_2},\ \ldots,\ f^8_{new_{19}}\ \} \end{aligned} \tag{5b}$$

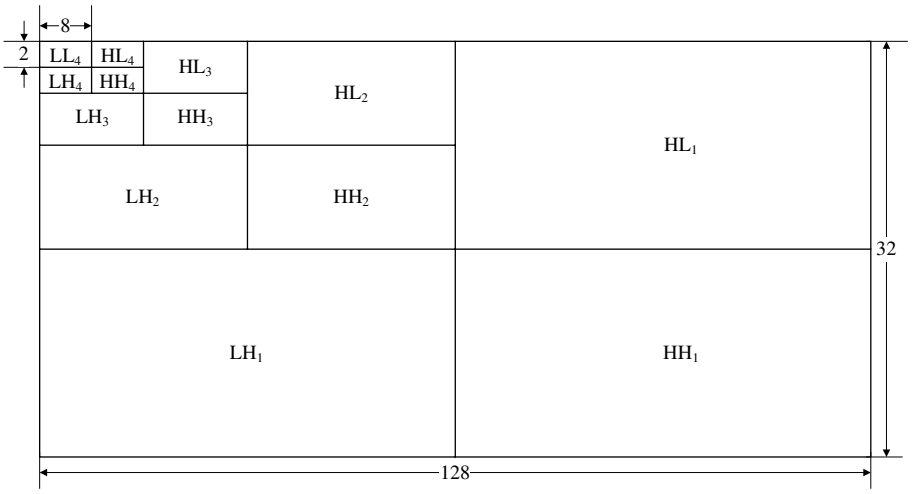

Fig. 5. Daubechies four level wavelet decomposition.

It may please to be noted that the proposed four level quantization is sufficient because we consider the both sign and magnitude information of wavelet coefficients. Higher number of quantization level increases the system performance but it also requires the more number of bits to represent the feature vector. Although, the increment of the system performance is not too significant. Our experimental results show no significant improvement with higher level of quantization compared to that of the four level quantization.

The 4-level quantization is shown in Figure 6(a). From Figure 6(a), we see that if the input value is greater than 0.5 then the output value is 11. The input values between 0.5 and 0 map onto the 10 output value. Similarly, for the negative input values 0 to -0.50 and -0.50 to -1.0 map onto the output values 01 and 00, respectively. Figure 6(b) shows a distribution example of the characteristic values of an extracted iris image. In Figure 6(b), $F(n)$ is the wavelet coefficient values and n is the number of characteristic values.

D. Feature Matching

In this sub section, we discuss our approach to feature matching. Our approach consists of setting rotation invariant feature vectors, assigning weight to a feature vector and finally the decision for a match. All these steps are discussed in following.

Rotation Invariant: It is observed that usually an iris is rotated within small angle [12]. So, to achieve the rotation invariant feature, we propose circularly shifting the normalized image in seven positions (-12, -8, -4, 0, 4, 8, 12 pixel) [12] in y- direction and hence storing the features at seven different angles. Shifting -12, -8, -4, 0, 4, 8, 12 pixels in y- direction means rotating the original eye in $-9^\circ, -6^\circ, -3^\circ, 0^\circ, 3^\circ, 6^\circ$ and 9°. Then the feature vector in each angel is represented by Equation (6).

$$
\begin{aligned}
{}_\theta F_{new} \quad = \quad & \{\ {}_\theta f^1_{new_1},\ {}_\theta f^1_{new_2},\ \ldots,\ {}_\theta f^1_{new_{19}}; \\
& {}_\theta f^2_{new_1},\ {}_\theta f^2_{new_2},\ \ldots,\ {}_\theta f^2_{new_{19}}; \\
& \ldots; \\
& {}_\theta f^8_{new_1},\ {}_\theta f^8_{new_2},\ \ldots,\ {}_\theta f^8_{new_{19}}\ \}
\end{aligned}
\tag{6}
$$

where, θ is an angle of rotation.

Matching: For matching, we assign a weight to each feature vector and also apply a weighted similarity measure procedure in our work. In order to achieve a higher accuracy of recognition rate, we assign a weight to each characteristic value. The main idea is to assign a higher value of weights to a feature which has more significance in the iris part.

We observed that upper and lower part of the iris is occluded by the eyelids and eyelashes in maximum cases. From our study we also observed that the most discriminating iris features are present in the iris region near to the pupil boundary. Hence, we apply a weighted matching procedure to compare the two feature vectors. Figure 7(b) is the eight sub divided regions in normalized image corresponding to iris structure which is shown in Figure 7(a). The maximum weight is given to that sub images which are more visible and the least weight is given to that sub images which are maximally occluded by eyelids and eyelashes. The weight assignment procedure is shown in Figure 7. In Figure 7, we see that the regions I_1 and I_3 are given maximum weight (1.0) because these regions are closer to the pupil boundary and are not obstructed by eyelashes or eyelids in majority of the cases. The I_5 and I_7 regions are far away from the pupil boundary but the chance of blocking by eyelashes or eyelids is comparatively low. So, we assign the second maximum weight (0.75) to the regions I_5 and I_7. The maximum chance of eyelashes and eyelids occlusion is in I_6 and I_8 regions and these regions are also far away from the pupil boundary. Hence, we assign the least weight (0.25) to these regions. The I_2 and I_4 regions are nearer to the pupil boundary but chance of occlusion by eyelashes and eyelids are high, so we assign 0.50 weight to these regions. We decide the above mentioned

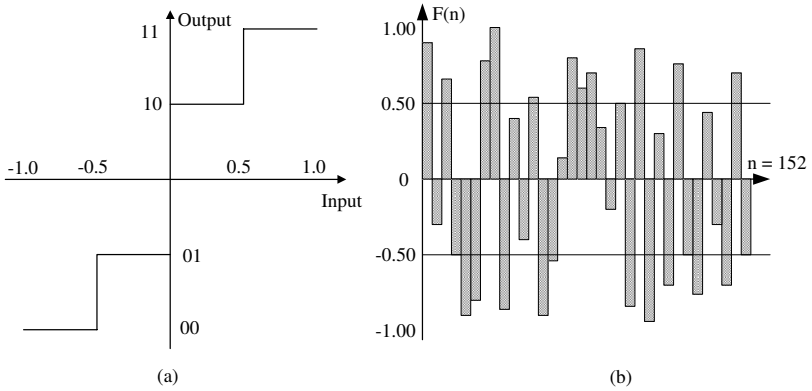

Fig. 6. Feature encoding procedure.

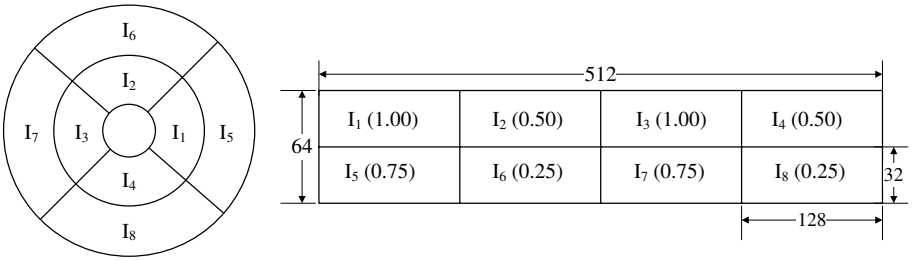

(a) Iris structure (b) Weight assignment in normalized sub images corresponding to (a)

Fig. 7. Weight assignment in eight subdivided iris blocks.

weight assignment empirically after a several run on the iris image databases used in our work.

The similarity measure is calculated by taking the weighted inner product we denote it as S of the weighted feature vector under test and each of the seven values of features corresponding to seven angles of rotation. We consider the minimum value among these seven product value as a similarity value. Equation (7) is used for calculating the inner product of two characteristic vectors.

$$S = \min_{\theta} \left\{ \frac{1}{152} \sum_{n=1}^{8} A_{I_n} \sum_{i=1}^{19} \frac{{}_{\theta}f_i^{'R^n} f_i^{'T^n}}{16} \right\} \tag{7}$$

where, ${}_{\theta}f_i^{'R^n}$ and $f_i^{'T^n}$ are the i-th feature of the n-th sub image in θ rotation corresponding to the feature vector of the user that has been already registered and the feature vector of the user that is generated from the iris image of the eye of the user, respectively. A_{I_n} is the weight corresponding to the sub image shown in Figure 7. A_{I_n} is defined in Equation (8).

$$A_{I_n} = \begin{cases} 1.00 & if \quad n = 1 \quad or \quad 3 \\ 0.75 & if \quad n = 5 \quad or \quad 7 \\ 0.50 & if \quad n = 2 \quad or \quad 4 \\ 0.25 & if \quad n = 6 \quad or \quad 8 \end{cases} \tag{8}$$

The ${}_{\theta}f_i^{'x}$ is defined in Equation 9.

$${}_{\theta}f_i^{'n} = \begin{cases} +4 & if \quad {}_{\theta}f_{new_i}^{n} = 11 \\ +1 & if \quad {}_{\theta}f_{new_i}^{n} = 10 \\ -1 & if \quad {}_{\theta}f_{new_i}^{n} = 01 \\ -4 & if \quad {}_{\theta}f_{new_i}^{n} = 00 \end{cases} \tag{9}$$
$$\text{where} \quad i = 1, 2, \ldots, 19 \quad \text{and} \quad n = 1, 2, \ldots, 8$$

According to the above mentioned principle, the positive values are added to the inner product S of the two characteristic vectors where the two characteristic vectors have the same-signed values with respect to each dimension. Otherwise, negative values are added to the inner product S of the two vectors. Consequently, the inner product S of the two characteristic vectors increases if the two data belong to the same person, while the inner product S of the two characteristic vectors decreases if the two data does not belong to the same person.

*Decision:*User authenticity is determined according to the measured similarity obtained from the, inner product S of the two characteristic vectors. The determination of the user authenticity using similarity measure depends on the following Equation (10).

$$Authenticity = \begin{cases} True & if \quad S > C \\ False & Otherwise \end{cases} \tag{10}$$

where C is a reference value for verifying the similarity between the two characteristic vectors. That is, if the inner

product S of the two characteristic vectors is equal or more than the verification reference value C, then the user is determined as an enrollee. Otherwise, the user is determined as an imposter.

IV. Experimental Results

We have implemented our approach using C programming language in Fedora Core 5 operating system environment with Intel *P4* processor, 1.7 GHz and 512 MB RAM. We use GNU compiler GCC version 4.1.0 for compiling and executing our program. For plotting graph we use GNU plot version 4.0.

Our approach has been tested with 1000 images of Bath [23], 1800 images of UBIRIS [24] and 450 images of MMU [25] iris image databases. We compare our approach with some best known algorithms [3], [8], [11], [9], [12], [6]. There are some reported results of these approaches however, those results are with CASIA [26] iris database. CASIA database is now obsolete because the CASIA database are hand-edited by painting the entire pupil with a circular disk of uniformly dark pixels and hence making the database trivial. To compare our work with the existing work, we have implemented the methodologies in the existing work and experimented with same set of databases.

Extensive experiments on different iris image databases are performed to evaluate the accuracy of the proposed method. The experiments are completed in two modes: identification (one-to-one) and verification (one-to-many). In identification mode, for a test sample, we make a one-to-many search of the entire database to find the most matched template with the test sample. If the test sample and the found template are from the same class, this is a correct recognition. Therefore, in identification mode, we can measure by *Correct Recognition Rate (CRR)*. The *Correct Recognition Rate (CRR)* is defined in Equation (11).

$$CRR = \frac{\text{Correctly recognized user number}}{\text{Total enrolled user number}} \times 100 \qquad (11)$$

In verification mode, assuming that a test sample is from a specified subject, we measure the performance in terms of three error rates: *False Acceptance Rate (FAR)*, *False Rejection Rate (FRR)* and *Equal Error Rate (ERR)*. These three measures are defined bellow.

- *False Acceptance Rate (FAR):* The probability of identifying an imposter as an enrolled user.
- *False Rejection Rate (FRR):* The probability of rejecting an enrolled user, as if he is an imposter.
- *Equal Error Rate (ERR):* ERR is the value where the FAR and FRR are equal.

Figure 8(a), 8(b) and 8(c) show the *FAR* and *FRR* curve for different threshold values (C) for MMU, Bath and UBIRIS iris databases, respectively. We calculate the ERR values for different iris databases from *FAR* and *FRR* curve. The *CRR*, *ERR* and number of bits required to store a feature vector for different method are listed in Table I. From Table I, we see that our approach provides a higher *CRR* and lower *ERR* and at the same time with a lesser number of bits required to store the feature vectors.

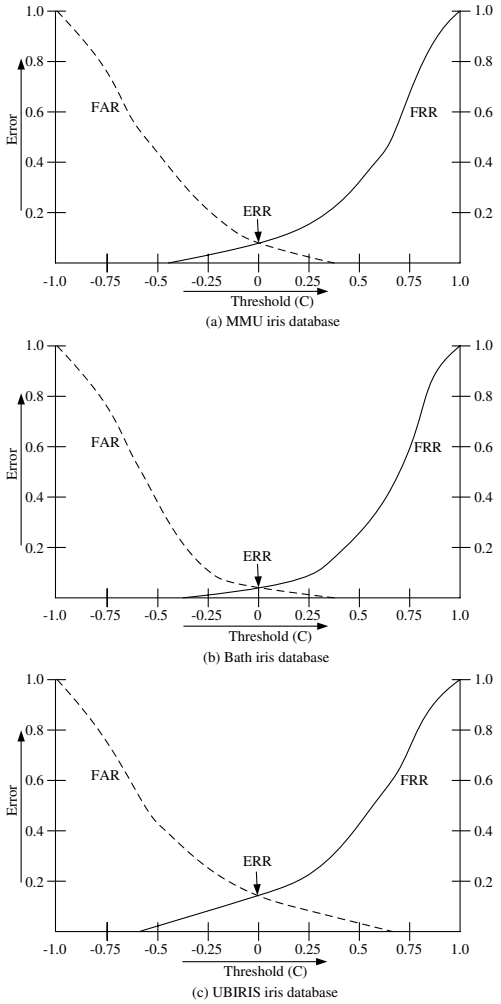

Fig. 8. FAR and FRR for different threshold values.

V. Conclusion

In this paper, we present a novel and efficient approach to extract iris features and matching technique to compare iris features. Our approach uses Daubechies wavelet transform with four coefficients. The Daubechies wavelet transform is easy to compute and fast compared to the other methods on texture analysis. Further, Daubechies wavelet transform allows to keep the count of feature vectors into a significantly lesser numbers. This is indeed without affecting the accuracy of the results. This way we are able to represent feature vectors with only 304 bits. Although Ali et al. [6] propose an approach to represent feature vectors with 87 bits but the accuracy rate is very poor. In addition to the savings in the number of feature vectors, another contribution in our approach is to assign a weight to each feature vector and hence to increase more accuracy in the similarity measure. Our approach is comparable to all existing approaches with respect to the number of bits to represent feature vectors and processing time. So far the accuracy rate is concerned our approach is also leads the existing approaches except the approach proposed

TABLE I
RECOGNITION RATE.

Methodology	Correct recognition rate (CRR) (%)			Equal error rate (ERR) (%)			Required bit to represent feature vector	Processing + matching time (ms)
	MMU	Bath	UBIRIS	MMU	Bath	UBIRIS		
Daugman [3]	99.25	99.37	98.12	0.24	0.25	0.98	2048	242.3
Wildes [8]	97.43	97.81	96.18	1.36	1.29	2.28	> 2048	233.5
Ma et al. [11]	95.33	96.22	92.44	1.88	1.76	8.22	1320	98.5
Ma et al. [9]	96.33	97.22	94.44	1.73	1.81	7.97	1280	102.1
Ma et al. [12]	96.43	96.71	92.86	1.65	1.74	7.92	1600	132.7
Ali et al. [6]	95.20	94.16	89.23	1.92	2.06	9.50	87	51.2
Proposed approach	98.87	99.13	97.12	0.79	0.31	1.27	304	72.3

by Daugman [3]. In fact, accuracy rate in our approach and Daugman approach is not remarkably differ. It also may be noted that Daugman's accuracy rate is at the expense of a higher number of computations and may be impractical for several online authentication systems.

ACKNOWLEDGMENT

The work is supported by Indian Institute of Technology Kharagpur under the scheme of Institute Sponsor to Innovative Research and Development (ISIRD).

REFERENCES

[1] J. G. Daugman. High Confidence Visual Recognition of Persons by a Test of Statistical Independence. *IEEE Transactions on Pattern Analysis and Machine Intelligence*, 15(11):1148–1161, November 1993.
[2] John Daugman. Iris Recognition. *American Scientist*, 89:326–333, July-August 2001.
[3] J. Daugman. How iris recognition works. *IEEE Transactions on Circuits and Systems for Video Technology*, 14(1):21– 30, 2004.
[4] W. W. Boles and B. Boashash. A Human Identification Technique Using Images of the Iris and Wavelet Transform. *IEEE Transaction on Signal Processing*, 46(4):1185–1188, 1998.
[5] M. Vasta, R. Singh, and A.Noore. Reducing the False Rejection Rate of Iris Recognition Using Textural and Topological Fearures. *International Journal of Signal Processing*, 2(2):66–72, 2005.
[6] Jafar M. H. Ali and Aboul Ella Hassanien. An Iris Recognition System to Enhance E-security Environment Based on Wavelet Theory. *AMO - Advanced Modeling and Optimization journal*, 5(2):93–104, 2003.
[7] Shinyoung Lim, Kwanyong Lee, Okhwan Byeon, and Taiyun Kim. Efficient Iris Recognition through Improvement of Feature Vector and Classifier. *ETRI Journal*, 23(2):61–70, June 2001.
[8] R. P. Wildes. Iris Recognition: An Emerging Biometric Technology. *Proceedings of the IEEE*, 85(9):1348–1363, September 1997.
[9] L. Ma, T. Tan, D. Zhang, and Y. Wang. Local Intensity Variation Analysis for Iris Recognition. *Pattern Recognition*, 37(6):1287–1298, 2004.
[10] L. Ma, Y. Wang, and T. Tan. Iris recognition based on multichannel gabor filtering. In *Proc. of the 5th Asian Conference on Computer Vision*, volume I, pages 279–283, 2002.
[11] Li Ma, Tieniu Tan, Yunhong Wang, and Dexin Zhang. Efficient Iris Recognition by Characterizing Key Local Variations. *IEEE Transactions on Image Processing*, 13(6):739–750, June 2004.
[12] L. Ma, T. Tan, Y. Wang, and D. Zhang. Personal Identification Based on Iris Texture Analysis. *IEEE Transaction on Pattern Analysis and Machine Intelligence*, 25(12):1519–1533, December 2003.
[13] Jaemin Kim, Seongwon Cho, Jinsu Choi, and II Robert J. Marks. Iris recognition using wavelet features. *J. VLSI Signal Process. Syst.*, 38(2):147–156, 2004.
[14] Y. Zhu, T. Tan, and Y. Wang. Biometric Personal Identification Based on Iris Patterns. In *Proc. of the 15th International Conference on Pattern Recognition*, volume II, pages 805–808, 2000.
[15] Tai Sing Lee. Image representation using 2d gabor wavelets. *IEEE Transactions on Pattern Analysis and Machine Intelligence*, 18(10):959–971, 1996.
[16] B. S. Manjunath and W. Y. Ma. Texture features for browsing and retrieval of image data. *IEEE Transactions on Pattern Analysis and Machine Intelligence*, 18(8):837–842, 1996.
[17] J. Shen, W. Shen, and D. F. Shen. On geometric and orthogonal moments. *International Journal of Pattern Recognition and Artificial Intelligence*, 14(7):875–894, 2000.
[18] L. Ma, Y. Wang, and T. Tan. Iris Recognition Using Circular Symmetric Filters. In *Proc. of the 16th International Conference on Pattern Recognition*, volume II, pages 414–417, 2002.
[19] J. Daugman. The importance of being random: Statistical principles of iris recognition. *Pattern Recognition*, 36(2):279–292, February 2003.
[20] S. Dey and D. Samanta. Efficient and accurate approach to iris segmentation. Technical report, School of Information Technology, July 2007.
[21] S. Mallat and W. Hwang. Singularity detection and processing with wavelets. *IEEE Transaction on Information Theory*, 38(2):617–643, 1992.
[22] A. Jensen and A. la Cour-Harbo. *Ripples in Mathematics: The Discrete Wavelet Transform*. Springer, 2001.
[23] University of Bath iris image database, 2007. http://www.bath.ac.uk/elec-eng/research/sipg/irisw.
[24] Hugo Proença and Luís A. Alexandre. Ubiris: A noisy iris image database. In Fabio Roli and Sergio Vitulano, editors, *ICIAP*, volume 3617 of *Lecture Notes in Computer Science*, pages 970–977. Springer, 2005.
[25] Multimedia University iris image database. http://pesona.mmu.edu.my/čcteo/.
[26] CASIA iris image database. http://www.sinobiometrics.com.